Isoscalar and Isovector Splitting of Pygmy Dipole Structures

N. Paar,[1,*] Y. F. Niu,[1,2] D. Vretenar,[1] and J. Meng[2,3]

[1]*Physics Department, Faculty of Science, University of Zagreb, Croatia*

[2]*State Key Laboratory for Nuclear Physics and Technology, School of Physics, Peking University, Beijing 100871, China*

[3]*School of Physics and Nuclear Energy, Beihang University, Beijing 100083, China*

(Received 14 April 2009; revised manuscript received 29 May 2009; published 17 July 2009)

The electric-dipole response of ^{140}Ce is investigated using the fully consistent relativistic quasiparticle random phase approximation. By analyzing the isospin structure of the $E1$ response, it is shown that the low-energy (pygmy) strength separates into two segments with different isospin character. The more pronounced pygmy structure at lower energy is composed of predominantly isoscalar states with surface-peaked transition densities. At somewhat higher energy the calculated $E1$ strength is primarily of isovector character, as expected for the low-energy tail of the giant dipole resonance. The results are in qualitative agreement with those obtained in recent (γ, γ') and $(\alpha, \alpha'\gamma)$ experiments, and provide a simple explanation for the splitting of low-energy $E1$ strength into two groups of states with different isospin structure and radial dependence of the corresponding transition densities.

DOI: 10.1103/PhysRevLett.103.032502 PACS numbers: 21.10.Gv, 21.30.Fe, 21.60.Jz, 24.30.Cz

Exotic modes of collective excitation represent unique structure phenomena in nuclear many-body systems with a pronounced asymmetry in the number of protons and neutrons [1]. A representative example is the pygmy dipole resonance (PDR), a low-energy mode that corresponds to a resonant oscillation of the weakly bound neutron skin against the isospin saturated proton-neutron core. Even though high-resolution data on low-energy dipole states have been obtained in recent (γ, γ') experiments [2–8], the details of the underlying nature and dynamics of the PDR remain largely unknown. Recent experiments with radioactive ion beams have extended the studies of low-lying dipole response towards exotic nuclear systems with pronounced neutron excess [9,10]. The occurrence of PDR has also been investigated using a variety of theoretical approaches and models [1]. More recent studies have made use of the quasiparticle RPA plus phonon coupling [11], the quasiparticle-phonon model [12], the relativistic RPA [13,14] and quasiparticle random phase approximation (QRPA) [15], as well as the relativistic quasiparticle time blocking approximation [16,17].

A recent $(\alpha, \alpha'\gamma)$ study of electric-dipole excitations below the particle threshold in the semimagic nucleus ^{140}Ce [2] has shown that the PDR structure separates into two parts. By comparing the observed low-lying strength to results from photon scattering experiments on the same target [8], it was noticed that the lower part of the PDR is excited both in $(\alpha, \alpha'\gamma)$ and (γ, γ') scattering, whereas the higher-energy component seems not to be excited by α particles.

In this Letter we analyze the isospin properties and transition densities of low-lying dipole excitations in ^{140}Ce. Similar aspects of the PDR will be considered as in Ref. [2], but from a theoretical point of view. The goal is to explore in simple terms, i.e., by analyzing the isotopic and spatial dependence of transition densities for dipole excitations, the splitting of the PDR structure into two groups of states, excited either by both the nuclear part of the α-nucleon interaction and photons, or only photons, respectively.

The present analysis uses the fully self-consistent relativistic quasiparticle random phase approximation (RQRPA) based on the relativistic Hartree-Bogoliubov model (RHB) [18]. Details of the formalism can be found in Refs. [1,18]. In the RHB + RQRPA model the effective interactions are implemented in a fully consistent way. In the particle-hole channel effective Lagrangians with density-dependent meson-nucleon couplings are employed [19], and pairing correlations are described by the pairing part of the finite-range Gogny interaction [20]. Both in the ph and pp channels, the same interactions are used in the RHB equations that determine the canonical quasiparticle basis, and in the matrix equations of the RQRPA.

The full set of RQRPA equations is solved by diagonalization. The result is excitation energies E_λ and the corresponding forward- and backward-going amplitudes, X^λ and Y^λ, respectively, that are used to evaluate the transition strength:

$$B_J^T(E_\lambda) = \frac{1}{2J_i+1}\Big|\sum_{\mu\mu'}\{X^{\lambda,J0}_{\mu\mu'}\langle\mu||\hat{Q}^T_J||\mu'\rangle + (-1)^{j_\mu - j_{\mu'}+J}Y^{\lambda,J0}_{\mu\mu'}\langle\mu'||\hat{Q}^T_J||\mu\rangle\}[u_\mu v_{\mu'} + (-1)^J v_\mu u_{\mu'}]\Big|^2, \quad (1)$$

where μ and μ' denote canonical single-nucleon states, and u, v are the corresponding occupation factors. Discrete spectra are averaged with a Lorentzian distribution of arbitrary width ($\Gamma = 1.5$ MeV in the present calculation), and the electric $E1$ response is calculated for the isovector dipole operator:

$$\hat{Q}_{1\mu}^{T=1} = \frac{N}{N+Z}\sum_{p=1}^{Z} r_p Y_{1\mu} - \frac{Z}{N+Z}\sum_{n=1}^{N} r_n Y_{1\mu}. \quad (2)$$

Particularly relevant for the present study are the neutron and proton radial transition densities $\delta\rho_{n,p}(r)$, which describe nucleon density fluctuations induced by an external field [21]. For instance, by analyzing if $\delta\rho_n(r)$ and $\delta\rho_p(r)$ for a particular state appear to be in phase over some extended region within the nuclear volume, states with predominant isoscalar structure can be identified in the RQRPA dipole strength distribution [Eq. (1)].

The solid curve in Fig. 1 represents the total RHB + RQRPA $E1$ transition strength for ^{140}Ce, calculated with the DD-ME2 [22] parametrization of the effective Lagrangian. In addition to the pronounced collective isovector giant dipole resonance (GDR) peaked at $\approx$15 MeV, we notice an enhancement of $E1$ strength in the low-energy region below the neutron threshold, indicated by the vertical arrow. This structure could be attributed to a PDR. The dotted, dashed, and dash-dotted curves illustrate the isospin structure of the $E1$ strength distribution. These curves connect states with predominant (at least 70%, 80%, and 90%, respectively) isoscalar components, identified by analyzing the corresponding proton and neutron transition densities over the radial interval [0, 8] fm. When for a particular state the proton and neutron transition densities are found to be in phase over more than 70% of this range of the radial coordinate, the state is denoted IS 70%, and analogously for the states IS 80% and IS 90%. For the low-energy excitations around the pronounced peak at 8.4 MeV the proton and neutron transition densities are in phase over more than 80% of the radial interval [0, 8] fm; i.e., these states are predominantly isoscalar. Some isoscalar states are also found at excitation energy $E > 10$ MeV, but in that interval, obviously, isovector collective motion dominates. The analysis of the isospin structure of the $E1$ transition strength in Fig. 1 indicates that most of the low-energy strength is of isoscalar character, and therefore sensitive to isoscalar probes such as α particles. States at higher energy, however, would probably not be excited in $(\alpha, \alpha'\gamma)$ experiments because of their predominant isovector character. Photon scattering, on the other hand, should excite dipole states over a broader low-energy interval, but (γ, γ') experiments have been restricted to the region below the neutron separation energy. Indeed, results of RQRPA calculations [1,15] indicate that part of the PDR strength may be missing in (γ, γ') experiments; i.e., these calculations predict PDR strength around and also above the neutron threshold. Some progress in recovering part of the unresolved $E1$ strength has already been reported [6], but future experimental studies across the neutron threshold may be necessary to account for the missing low-lying $E1$ strength.

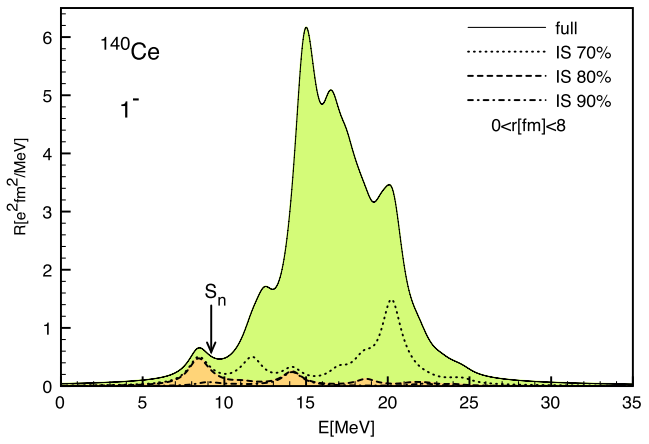

FIG. 1 (color online). The total RHB + RQRPA $E1$ transition strength for ^{140}Ce (solid curve). The dotted, dashed, and dash-dotted curves connect states with predominant (at least 70%, 80%, and 90%, respectively) isoscalar (IS) components, identified by analyzing the corresponding proton and neutron transition densities over the radial interval [0, 8] fm. The vertical arrow denotes the one-neutron separation energy $S_n = 9.2$ MeV.

The photon field interacts with a nucleus as a whole, whereas α particles interact mainly with the nuclear surface, inducing isoscalar transitions with surface-peaked transition densities. It is, therefore, interesting to analyze in more detail the radial structure of the transition densities for the dipole states shown in Fig. 1. When the identification of states with predominant isoscalar components is based on the behavior of the corresponding neutron and proton transition densities in the radial interval [0, 4.25] fm, i.e., in the volume of the nucleus, one finds that these states are distributed over a wide energy region, but not below $E \approx 10$ MeV. Figure 2, on the other hand, displays the same analysis of the $E1$ transition strength, but the predominantly isoscalar states are identified by considering the in-phase or out-of-phase behavior of the corresponding neutron and proton transition densities in the surface region $4.25 < r < 8$ fm. In this case transitions with predominant isoscalar character are located mainly

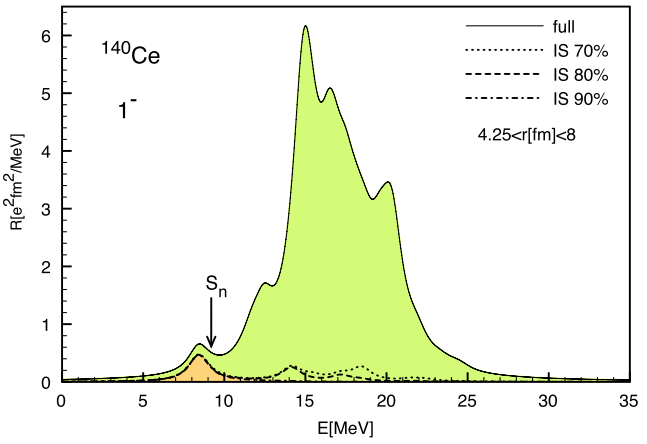

FIG. 2 (color online). Same as in Fig. 1, but the dotted, dashed, and dash-dotted curves are determined from the radial dependence of the neutron and proton transition densities in the surface region: $4.25 < r < 8$ fm.

in the low-energy region below 10 MeV. One can conclude that the low-energy isoscalar structure peaked at 8.4 MeV corresponds mainly to surface excitations. Low-lying isoscalar states with surface-peaked transition densities are precisely those expected to be induced in α-scattering experiments.

In Fig. 3 we plot the neutron and proton transition densities for the peaks at 8.4 MeV and 15.1 MeV. For the main peak at 15.1 MeV the transition densities display a radial dependence that is characteristic for the isovector GDR: the proton and neutron densities oscillate with opposite phases. The dynamics of the state at 8.4 MeV is different: the proton and neutron transition densities are in phase in the nuclear interior, and there is almost no contribution from the protons in the surface region. This low-energy state does not belong to statistical $E1$ excitations sitting on the tail of the GDR. Figure 4 explores in more detail the structure of the transition matrix elements for the PDR state at 8.4 MeV. The matrix elements [i.e., each term in the sum over μ and μ' in Eq. (1), representing the contribution of the corresponding $2qp$ configuration to the transition strength] are plotted as a function of the unperturbed energy of the corresponding $2qp$ configurations. Proton and neutron matrix elements are displayed separately. First, we note that the state at 8.4 MeV is characterized by a coherent superposition (matrix elements of the same sign) of more than ten neutron $2qp$ configurations. The largest matrix elements correspond to the following neutron transitions (in order of increasing $2qp$ unperturbed energy): $3s_{1/2} \rightarrow 3p_{3/2}$, $2d_{3/2} \rightarrow 3p_{3/2}$, $3s_{1/2} \rightarrow 3p_{1/2}$, $2d_{3/2} \rightarrow 3p_{1/2}$, $1h_{11/2} \rightarrow 1i_{13/2}$, $2d_{5/2} \rightarrow 3p_{3/2}$, $1g_{7/2} \rightarrow 1h_{9/2}$, $1h_{11/2} \rightarrow 2g_{9/2}$, $1g_{7/2} \rightarrow 2f_{5/2}$. Second, from the analysis of the QRPA amplitudes $(X^{\lambda}_{2qp})^2 - (Y^{\lambda}_{2qp})^2$ it follows that the total contribution of proton $2qp$ excitations to the state at 8.4 MeV is only 9%, well below the ratio Z/N expected for a GDR state, whereas 91% of the total amplitude corresponds to neutron transitions.

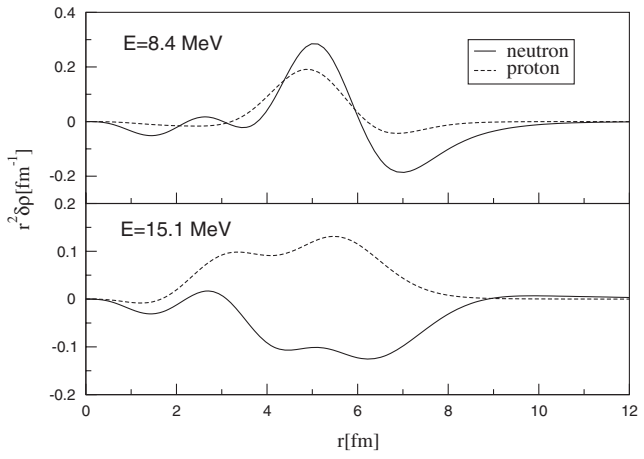

FIG. 3. The RQRPA neutron and proton transition densities for the peaks at 8.4 MeV and 15.1 MeV excitation energy in ^{140}Ce.

The relativistic QRPA accurately reproduces experimental excitation energies of the GDR, whereas the calculated PDR are only in qualitative agreement with available data. In the particular example of ^{140}Ce, the predicted PDR structure is calculated more than 2 MeV above the pygmy structure seen in (γ, γ') and $(\alpha, \alpha'\gamma)$ experiments [2]. The principal reason for this discrepancy lies in the fact that relativistic mean-field effective interactions, e.g., DD-ME2, have relatively low effective nucleon masses, typically $m^* < 0.7m_N$, where m_N denotes the free nucleon mass. A larger effective mass, i.e., a higher density of states around the Fermi surface, would lower the excitation energy of states with predominant isoscalar components, e.g., the PDR. Unfortunately, it is not simple to increase the effective nucleon mass in relativistic mean-field models, because this quantity is strongly constrained by the Dirac mass, which represents a measure of the strength of the spin-orbit single-nucleon potential [23,24]. In addition, our study is limited to a simple QRPA and does not include effects of coupling to low-energy surface phonons. This coupling will also enhance the effective nucleon mass. The analysis of PDR can be extended by introducing the coupling of two-quasiparticle excitations to collective vibrations, e.g., using the quasiparticle-phonon model [12], or the relativistic quasiparticle time blocking approximation [16]. In Ref. [16] it has been shown that the effect of two-phonon admixtures is a small shift of PDR states ($\leq$1 MeV) to lower excitation energies, but although the PDR calculated in the extended space contains sizable two-phonon admixtures, it basically retains a one-phonon character and the pygmy dynamics is not modified by the coupling to low-energy surface vibrations.

To illustrate how sensitive PDR is to the effective nucleon mass, in Fig. 5 we display the fully self-consistent RQRPA $E1$ strength calculated with the DD-ME2 interaction, in comparison to the $E1$ strength obtained with the same effective interaction, but with DD-ME2 neutron single-particle energies below and above the $N = 82$ shell

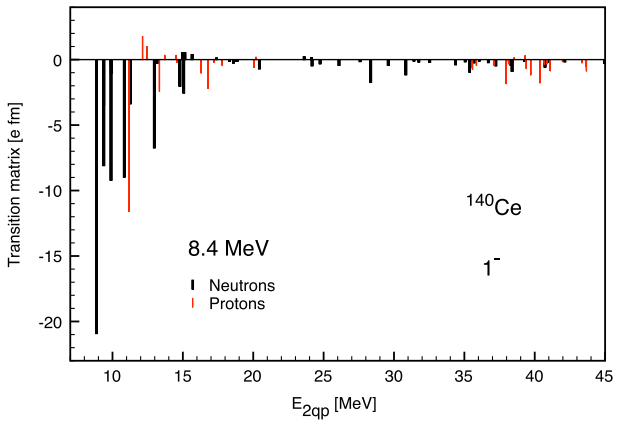

FIG. 4 (color online). The RQRPA neutron and proton transition matrix elements for the state at 8.4 MeV in ^{140}Ce, as a function of the unperturbed energy of the corresponding $2qp$ configurations.

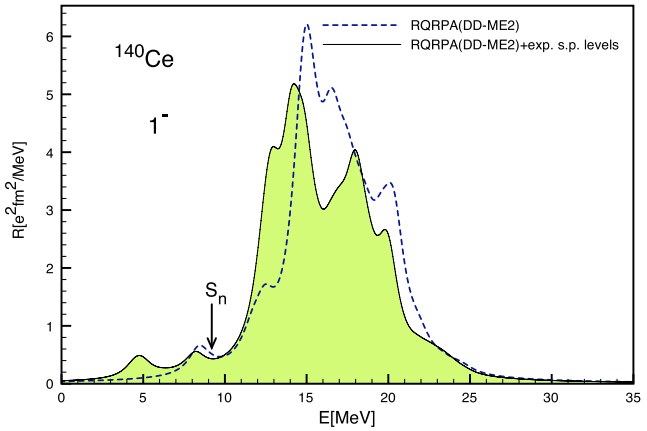

FIG. 5 (color online). The total RHB + RQRPA $E1$ transition strength for ^{140}Ce in comparison with calculation using experimental neutron single-particle energies.

gap replaced with experimental values. The empirical $N = 82$ gap is much smaller than the one predicted by DD-ME2; i.e., the empirical effective neutron mass is larger. By using experimental neutron single-particle energies one takes into account, at least on the level of single-nucleon energies, the effect of coupling to collective vibrations, but of course, the calculation is no longer self-consistent. Nevertheless, we notice that the enhancement of the effective neutron nucleon mass has a pronounced effect especially on the PDR structure. The $E1$ strength below 10 MeV is fragmented into two structures, with the lower one centered at $\approx$5 MeV and higher one peaked at $\approx$8 MeV, in much better agreement with data [2]. An analysis of the isospin content of these structures, based on proton and neutron transition densities, shows that isoscalar components are more pronounced in the lower structure at $\approx$5 MeV. We have also verified that the same pattern is calculated for ^{132}Sn, when DD-ME2 single-nucleon energies are replaced by empirical values.

In conclusion, the fully consistent relativistic QRPA has been used to calculate the electric-dipole response of ^{140}Ce. An analysis of the isospin structure of $E1$ strength, based on the radial dependence of the microscopic proton and neutron transition densities, has shown that the low-energy strength separates into two segments with qualitatively different isospin character. The more pronounced PDR structure at lower energy is composed of predominantly isoscalar states with surface-peaked transition densities. At energies above the main PDR peak the $E1$ strength is primarily of isovector character, with non-surface-peaked transition densities, as expected for the low-energy tail of the giant dipole resonance. The results are in qualitative agreement with those obtained in recent (γ, γ') and $(\alpha, \alpha'\gamma)$ experiments, and provide a simple explanation for the splitting of low-energy $E1$ strength into two groups of states, excited either by both the nuclear part of the α-nucleon interaction and photons, or only by photons, respectively.

This work was supported by the Unity through Knowledge Fund (UKF Grant No. 17/08) and MZOS—Project No. 1191005-1010. Y. F. Niu acknowledges support from the National Foundation for Science, Higher Education, and Technological Development of the Republic of Croatia. The work of J. M. and D. V. was supported in part by the Chinese-Croatian project ''Nuclear Structure Far from Stability.''

*npaar@phy.hr

[1] N. Paar, D. Vretenar, E. Khan, and G. Colò, Rep. Prog. Phys. **70**, 691 (2007).
[2] D. Savran, M. Babilon, A. M. van den Berg, M. N. Harakeh, J. Hasper, A. Matic, H. J. Wörtche, and A. Zilges, Phys. Rev. Lett. **97**, 172502 (2006).
[3] D. Savran *et al.*, Phys. Rev. Lett. **100**, 232501 (2008).
[4] S. Volz, N. Tsoneva, M. Babilon, M. Elvers, J. Hasper, R.-D. Herzberg, H. Lenske, K. Lindenberg, D. Savran, and A. Zilges, Nucl. Phys. **A779**, 1 (2006).
[5] R. Schwengner *et al.*, Phys. Rev. C **78**, 064314 (2008).
[6] B. Özel *et al.*, arXiv:0901.2443v1.
[7] B. Özel *et al.*, Nucl. Phys. **A788**, 385 (2007).
[8] A. Zilges *et al.*, Phys. Lett. B **542**, 43 (2002).
[9] P. Adrich *et al.*, Phys. Rev. Lett. **95**, 132501 (2005).
[10] O. Wieland *et al.*, Phys. Rev. Lett. **102**, 092502 (2009).
[11] D. Sarchi, P. F. Bortignon, and G. Coló, Phys. Lett. B **601**, 27 (2004).
[12] N. Tsoneva and H. Lenske, Phys. Rev. C **77**, 024321 (2008).
[13] J. Piekarewicz, Phys. Rev. C **73**, 044325 (2006).
[14] J. Liang, L. G. Cao, and Z. Y. Ma, Phys. Rev. C **75**, 054320 (2007).
[15] N. Paar, T. Nikšić, D. Vretenar, and P. Ring, Phys. Lett. B **606**, 288 (2005).
[16] E. Litvinova, P. Ring, and D. Vretenar, Phys. Lett. B **647**, 111 (2007).
[17] E. Litvinova, P. Ring, and V. Tselyaev, Phys. Rev. C **78**, 014312 (2008).
[18] N. Paar, P. Ring, T. Nikšić, and D. Vretenar, Phys. Rev. C **67**, 034312 (2003).
[19] N. Paar, T. Nikšić, D. Vretenar, and P. Ring, Phys. Rev. C **69**, 054303 (2004).
[20] J. F. Berger, M. Girod, and D. Gogny, Comput. Phys. Commun. **63**, 365 (1991).
[21] F. E. Serr, T. S. Dumitrescu, T. Suzuki, and C. H. Dasso, Nucl. Phys. **A404**, 359 (1983).
[22] G. A. Lalazissis, T. Nikšić, D. Vretenar, and P. Ring, Phys. Rev. C **71**, 024312 (2005).
[23] D. Vretenar, T. Nikšić, and P. Ring, Phys. Rev. C **65**, 024321 (2002).
[24] T. Nikšić, D. Vretenar, and P. Ring, Phys. Rev. C **72**, 014312 (2005).